International Journal of Engineering Inventions
e-ISSN: 2278-7461, p-ISSN: 2319-6491
Volume 12, Issue 6 [June. 2023] PP: 97-102

Numerical study on liquid cooling of Lithium-ion Battery pack

Nguyen ThiThanh Hoa[1], LuuKieu Oanh[2*]
[1,2]*Faculty of Vehicle and Energy Engineering, Thai Nguyen University of Technology, Thai Nguyen, Vietnam*

ABSTRACT:
Lithium-ion batteries are widely used in consumer electronics and are among the most favoured rechargeable batteries for applications such as portable devices, military usage, electric vehicles, and aerospace applications. However, lithium-ion batteries will be accompanied by a lot of heat during the charging and discharging process. It is easy to lead to the accumulation of heat inside the battery and then affect battery performance and safety if the heat is not dissipated timely. Therefore, in order to make the battery power system available to play a better performance while ensuring security, it is necessary to optimize the design of the battery cooling solution. In this study, the thermal behaviour of Lithium-ion battery packs is numerically investigated. The thermal management of the cells in the module is achieved based on forced water cooling. The computations of the temperature distribution in the module are performed with a three-dimensional modelling approach. The influences of discharge C-rate and inlet velocity on the thermal behaviour of the battery pack are analyzed. The result indicated that the maximum temperature at discharge rates of 2C and 3C are 300.02°K and 300.35°K. Moreover, increasing the inlet velocity results in a decrease in the maximum temperature of the cells.
KEYWORDS: *Electric vehicle; lithium-ion battery pack; water cooling strategies; ANSYS Fluent.*

Date of Submission: 02-06-2023 Date of acceptance: 12-06-2023

I. INTRODUCTION

A battery is an energy source which is used to convert chemical energy to electrical energy that can be extracted at a certain voltage. This electricity is generated from the electrochemical reduction-oxidation (redox) reactions within the active electrode materials. These reactions cause a continuous transfer between the anode (negative electrode) and cathode (positive electrode) of ions via an electrolyte and of electrons via an external circuit. The reacting substances (active materials) are usually integrated with the electrodes. During the discharge of the battery, the active material in the anode gets oxidized and releases electrons to the external circuit, whereas the active material in the cathode gets reduced by accepting the electrons. Electrochemical batteries are classified as primary (non-rechargeable) and secondary batteries (rechargeable) depending on the capability of being electrically recharged. After discharge, a secondary battery is recharged by applying electric current in the opposite direction of discharge. Lithium-ion batteries are widely used in consumer electronics and are among the most favoured rechargeable batteries for applications such as portable devices, military usage, electric vehicles, and aerospace applications [1]. They offer numerous advantages, including high energy density, minimal self-discharge, absence of memory effect (reduced capacity after repeated charging), high cell voltage, and specific energy.

As part of the energy of electric vehicles, power battery has a significant impact on vehicle performance. Because of the merits of small size, high power density, high voltage, low self-discharge and low resistance, lithium-ion batteries are widely used in the power system and obtain a lot of notice from many automobile manufacturers. In the general case, there is small space available for a power battery while designing the car. In addition, lithium-ion batteries will be accompanied by a lot of heat during the charging and discharging process. It is easy to lead to the accumulation of heat inside the battery and then affect battery performance and safety if the heat is not dissipated timely. If the heat dissipates unevenly, it will cause a large temperature difference inside the battery pack. The unevenness of the battery pack temperature field will cause unbalance of the battery modules and each cell's performance, and finally, affect the performance of the entire battery pack and security. Therefore, in order to make the battery power system available to play a better performance while ensuring security, it is necessary to optimize the design of the battery cooling solution. Therefore, battery thermal management systems (BTMSs) are required to dissipate the heat from the battery in time [2]. In the last decades, several types of BTMSs have been developed. Depending on the type of cooling medium, BTMSs can be categorized into four primary categories: an air cooling system (ACS) [3], a liquid cooling system [4], a phase-change-material (PCM) cooling system [5], and a heat pipe cooling system [6].

In this study, the thermal behaviour of Lithium-ion battery pack is numerically investigated. The thermal management of the cells in the module is achieved based on forced water cooling. The computations of the temperature distribution in the module are performed with a three-dimensional modelling approach. The influences of discharge C-rate and inlet velocity on the thermal behaviour of the battery pack are analyzed. The result indicated that the maximum temperature at discharge rates of 2C and 3C are 300.02°K and 300.35°K. Moreover, increasing the inlet velocity results in a decrease in the maximum temperature of the cells.

II. COMPUTATIONAL DOMAIN AND GOVERNING EQUATIONS

A calculation model is created, as shown in Figure 1. The battery pack consists of two rows of 18650 batteries. Each row contains four batteries. The battery thermos-physical parameters are shown in Table 1 [7]. Along the liquid flow direction, the cooling liquid just entering the battery pack conducts cooling liquid convection heat transfer on the battery surface, cooling the front module and heating the liquid itself; its cooling ability decreases, thus the temperature of the rear module will be higher than the front.

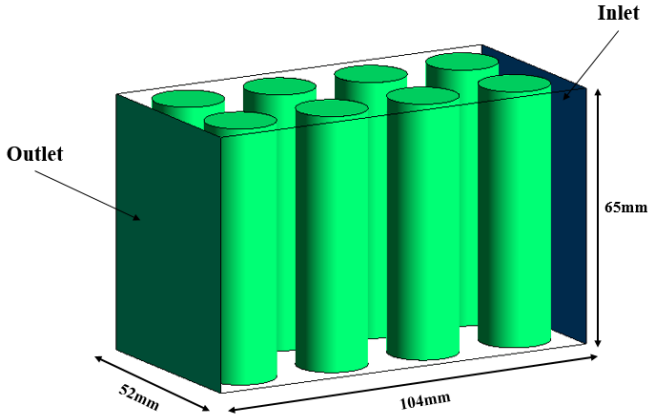

Figure 1. 3D computational model of battery pack module

Table 1. Physical and thermal properties of the 18650 li-ion battery.

Rated Voltage (V)	3.6	Specific Heat Capacity ($J.kg^{-1}K^{-1}$)	1200	Density ($kg.m^3$)	2722
Length	65	Diameter (mm)	18	Anisotropic thermal conductivity ($W.m^{-1}K^{-1}$)	$k_r = 0.2$ $k_z = 37.6$

The computational domain is discretized using structured hexahedral mesh elements (Figure 2a). The grid is clustered near the wall vicinity of batteries in order to take into account the strong gradients in this region. The middle plane of the battery module, where it was used to take place results, is shown in Figure 2b.

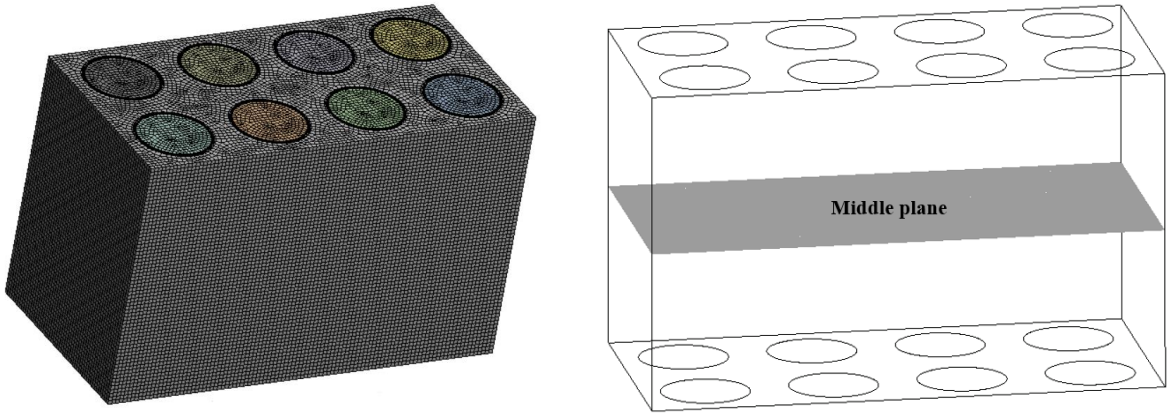

(a) (b)

Figure 2. a) Close-up of mesh elements of battery pack; b) The middle plane of computational domain

In ANSYS-Fluent, the governing equations include the continuity, momentum, and energy equations. For the cooling liquid, these equations are shown as:

Continuity equation:

$$\frac{\partial \rho}{\partial t} + \nabla(\rho u) = 0 \quad (1)$$

Momentum equation:

$$\rho\frac{\partial u}{\partial t}+\rho u.\nabla u=-\nabla p+\eta\nabla^2 u \quad (2)$$

Energy equation:

$$\frac{\partial(\rho c_p T)}{\partial t}+\nabla\left(\rho c_p u T\right)=\nabla(k\nabla T) \quad (3)$$

For the battery cell, the energy governing equation is expressed by:

$$\rho c_p\frac{\partial T}{\partial t}=\nabla(k\nabla T)+q \quad (4)$$

where ρ, c_p, T, p, k and q denote the density, specific heat, temperature, pressure, heat conductivity coefficient, the heat generation rate per unit volume of the battery, respectively.

A battery is considered as uniform a heat source. The heat generation rate per unit volume is expressed as equation 5.

$$q = a_0 + a_1 t + a_2 t^2 + \ldots + a_n t^n \quad (5)$$

Where $\boldsymbol{a_0}$~$\boldsymbol{a_n}$ are coefficients corresponding to the polynomial fitting method, q (W/m^3) is the heat generation rate and t (sec) is the time passed. These values were taken from [8]. The heat generation model is defined as an energy source term incorporated into CFD simulation using a user-defined function (UDF).

The standard k-ε model is selected which has been widely validated in modeling general low-speed and low-pressure flow around obstacles [9]. The k-ε turbulence model includes two equations for the turbulent kinetic energy k and the turbulent kinetic energy dissipation rate ε.

Turbulent kinetic energy equation:

$$\frac{\partial}{\partial t}(\rho k)+\frac{\partial}{\partial xj}(\rho k u j)=\frac{\partial}{\partial xj}\left(\left(\mu+\frac{\mu t}{\alpha k}\right)\frac{\partial k}{\partial xj}\right)+Gk+Gb-\rho\varepsilon-YM+Sk \quad (6)$$

Turbulent kinetic energy dissipation equation:

$$\frac{\partial}{\partial t}(\rho\varepsilon)+\frac{\partial}{\partial xj}(\rho\varepsilon u j)=\frac{\partial}{\partial xj}\left(\left(\mu+\frac{\mu t}{\alpha\varepsilon}\right)\frac{\partial\varepsilon}{\partial xj}\right)+C1\varepsilon\frac{\varepsilon}{k}(Gk+C3\varepsilon Gb)-\rho C2\varepsilon\frac{\varepsilon^2}{k}+S\varepsilon \quad (7)$$

where k and ε denote turbulent kinetic energy and turbulent dissipation rate, respectively.

The settings for the boundary conditions are as the following. The inlet and outlet are set as the velocity inlet and the pressure outlet, respectively. The top, bottom and two sides of the computational domain are defined as walls. In addition, the interfaces between batteries and fluid are defined as coupled walls.

The convergence criterion, i.e., the scaled residual, for both mass, momentum and energy equations are set to 10-5 and 10-6, respectively, in each time step of the flow.

To analyze mesh independency, three mesh sizes are tested: 253.500, 507.000 and 1100.000 elements. The mesh density was almost doubled in each refinement. The second one (507.000 elements) is used in the simulation (Fig. 2a)

The effects of time steps on the results are also tested using 50, 150 and 200 steps per cycle. Finally, 150 steps per cycle are used for the simulation in the transient regime.

IV. RESULTS AND DISCUSSION

Figure 3 shows the streamlines of the battery module. It can be seen that the flow resistance and the turbulence degree are big, and the heat transfer capacity of the battery and cooling liquid flow increase, which improves the cooling performance of the pack. Moreover, the whole battery pack is surrounded by the cooling liquid evenly and has a good heat exchange capability.

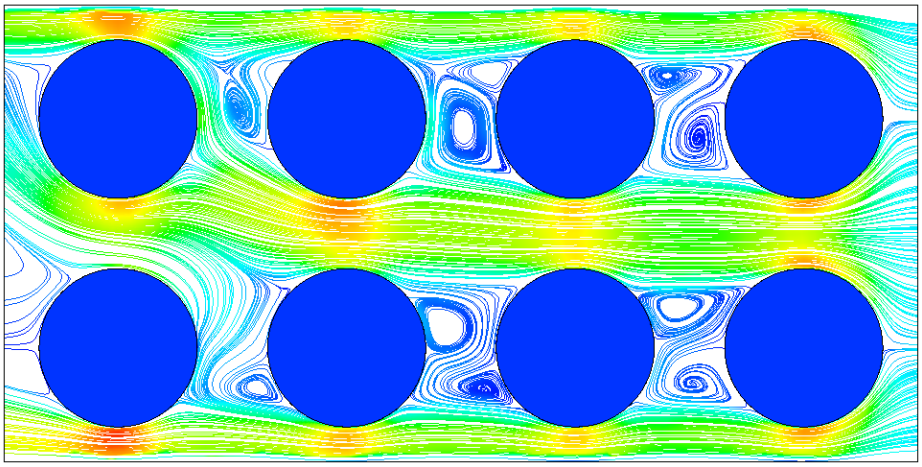

Figure 3. Streamlines of battery pack

The maximum temperatures of the battery pack of discharge for different C-rates are shown in Figure 4. It is obvious that the maximum cell temperature during 2C and 3C are increased. By checking Fig. 4's temperature plots, it is concluded that the battery with the maximum temperature is the nearest one to the fluid inlet, and the coolest battery is placed nearest to the fluid outlet. It can be noticed that the eddies behind the batteries have a clear impact on the temperature distribution; or other words, there exists a significant coupling of mass transfer with heat transfer.

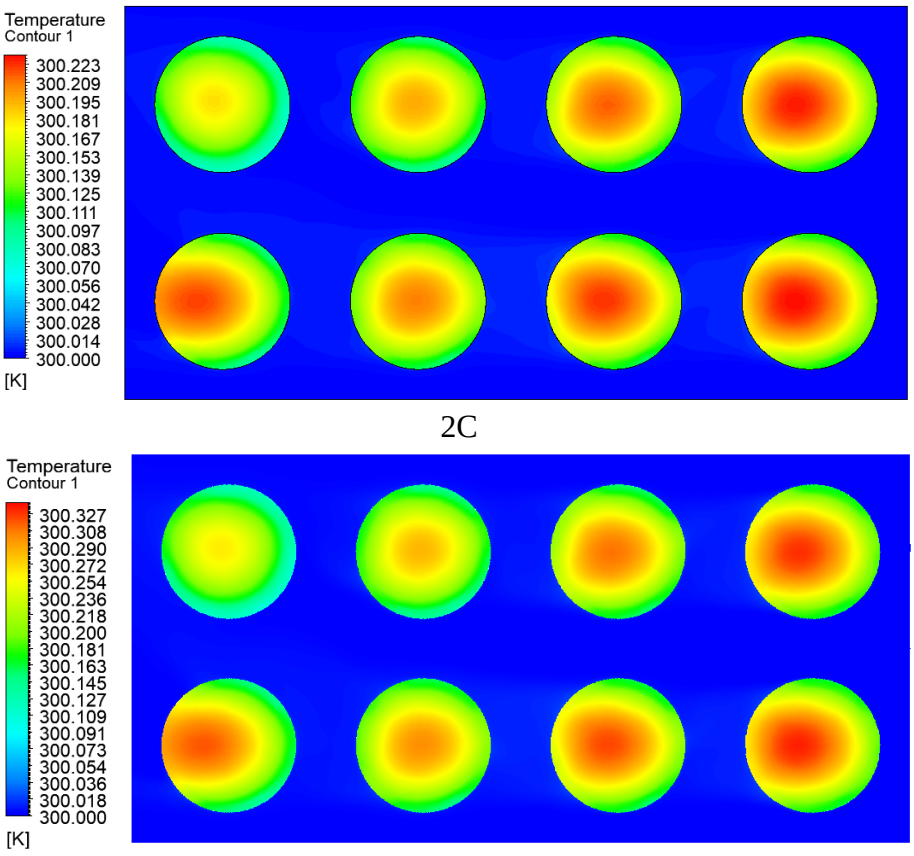

Figure 4. The evolution and distribution of temperature in battery pack through discharge under different C-rates.

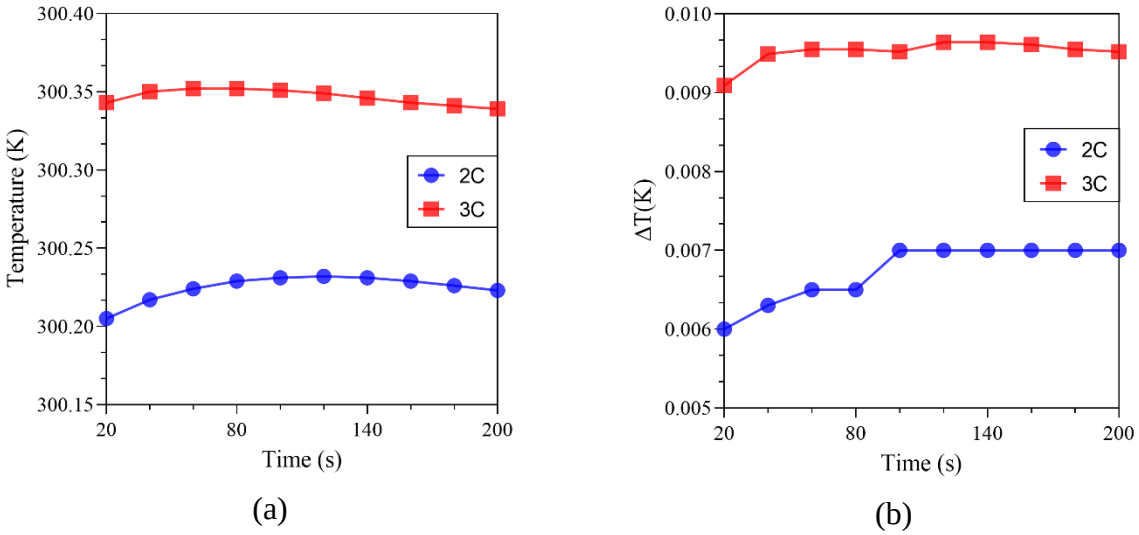

Figure 5. Temperature of the battery pack at different discharge rate.

The battery will generate more heat at a higher discharge rate. Figure 5 shows the maximum temperature difference of the battery pack discharge at 2 and 3 C. The inlet temperature of cooling water is 300°K. When the discharge rate of the battery increases from 2 to 3 C, the maximum temperature of the battery increases from 300.223°K to 300.35°K (it is noted here that the time for simulation is only 200s, so the difference of maximum temperature value is very small). As the battery temperature increases, the cooling water takes away more heat, resulting in an increase in the outlet temperature of the water. The increase in the temperature difference between the inlet and outlet will increase the temperature difference of the battery pack, as shown in Figure 5b. In the immersion cooling system, due to sufficient heat exchange between the water and the battery, the temperature difference between the inlet temperature and the outlet temperature is large, thus increasing the temperature difference of the battery pack.

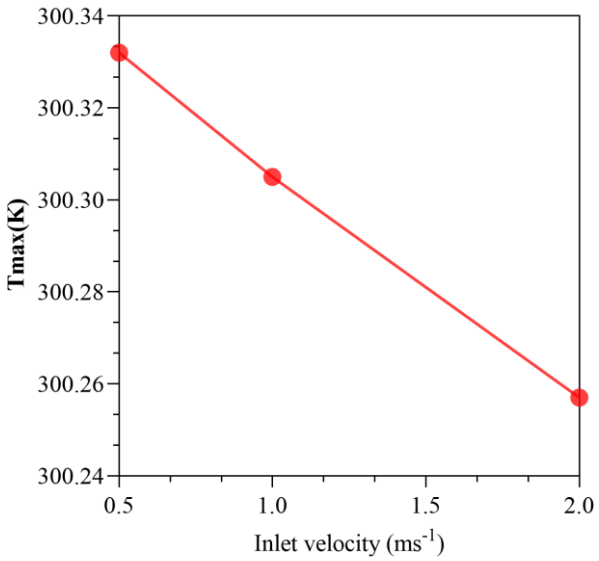

Figure 6. Variation of maximum temperature with different inlet velocity

Figure 6 demonstrates the maximum temperature of the battery with different inlet velocities for discharge rate = 3C. Specifically, the Tmax reduces with the rise of the inlet velocity. The reason is that a higher inlet velocity leads to an increase the heat transfer between the battery and the water.

V. CONCLUSION

The purpose of this study is to investigate the effect of a water immersion cooling system of lithium-ion batteries. A numerical model is established to study the influence of key parameters on the cooling performance of the system. As the battery is in direct contact with the cooling water, the heat transfer effect is

greatly improved, and the cooling performance of the system is enhanced. The main conclusions of this work can be summarized as follows:

- For the same inlet velocity, the maximum temperature at discharge rates of 2C and 3C are 300.02°K and 300.35°K.

- Increasing the inlet velocity results in a decrease in the maximum temperature of the cells.

- In the immersion cooling system, due to sufficient heat exchange between the water and the battery, the temperature difference between the inlet temperature and the outlet temperature is large, thus increasing the temperature difference of the battery pack.

Acknowledgment

The authors would like to express our gratitude to the Thai Nguyen University of Technology for support of this work.

REFERENCES

[1]. Chen, Y., Kang, Y., Zhao, Y., Wang, L., Liu, J., Li, Y., Liang, Z., He, X., Li, X., Tavajohi, N., and Li, B., 2021, "A Review of Lithium-Ion Battery Safety Concerns: The Issues, Strategies, and Testing Standards," Journal of Energy Chemistry, 59, pp. 83–99.

[2]. Lu, L., Han, X., Li, J., Hua, J., and Ouyang, M., 2013, "A Review on the Key Issues for Lithium-Ion Battery Management in Electric Vehicles," Journal of Power Sources, 226, pp. 272–288.

[3]. Fan, L., Khodadadi, J. M., and Pesaran, A. A., 2013, "A Parametric Study on Thermal Management of an Air-Cooled Lithium-Ion Battery Module for Plug-in Hybrid Electric Vehicles," Journal of Power Sources, 238, pp. 301–312.

[4]. Panchal, S., Khasow, R., Dincer, I., Agelin-Chaab, M., Fraser, R., and Fowler, M., 2017, "Thermal Design and Simulation of Mini-Channel Cold Plate for Water Cooled Large Sized Prismatic Lithium-Ion Battery," Applied Thermal Engineering, 122, pp. 80–90.

[5]. Rao, Z., and Wang, S., 2011, "A Review of Power Battery Thermal Energy Management," Renewable and Sustainable Energy Reviews, 15(9), pp. 4554–4571.

[6]. Putra, N., Ariantara, B., and Pamungkas, R. A., 2016, "Experimental Investigation on Performance of Lithium-Ion Battery Thermal Management System Using Flat Plate Loop Heat Pipe for Electric Vehicle Application," Applied Thermal Engineering, 99, pp. 784–789.

[7]. Behi, H., Karimi, D., Behi, M., Ghanbarpour, M., Jaguemont, J., Sokkeh, M. A., Gandoman, F. H., Berecibar, M., and Mierlo, J. V., 2020, "A New Concept of Thermal Management System in Li-Ion Battery Using Air Cooling and Heat Pipe for Electric Vehicles," Applied Thermal Engineering, 174, p. 115280.

[8]. Hwang, F. S., Confrey, T., Scully, S., Callaghan, D., Nolan, C., Kent, N., and Flannery, B., 2020, "MODELLING OF HEAT GENERATION IN AN 18650 LITHIUM-ION BATTERY CELL UNDER VARYING DISCHARGE RATES," Proceeding of 5th Thermal and Fluids Engineering Conference (TFEC), Begellhouse, New Orleans, LA, USA, pp. 333–341.

[9]. Xing, J., Liu, Z., Huang, P., Feng, C., Zhou, Y., Zhang, D., and Wang, F., 2013, "Experimental and Numerical Study of the Dispersion of Carbon Dioxide Plume," Journal of Hazardous Materials, 256–257, pp. 40–48.